Open Research Online

The Open University's repository of research publications
and other research outputs

Phosphorus recycling in photorespiration maintains high photosynthetic capacity in woody species

Journal Item

For guidance on citations see FAQs.

Version: Accepted Manuscript

Link(s) to article on publisher's website:
http://dx.doi.org/doi:10.1111/pce.12468

oro.open.ac.uk

Phosphorus recycling in photorespiration maintains high photosynthetic capacity in woody species

DAVID S. ELLSWORTH[1,*], KRISTINE Y. CROUS[1], HANS LAMBERS[2], JULIA COOKE[1,3]

[1] *Hawkesbury Institute for the Environment, Locked Bag 1797, University of Western Sydney, Penrith, NSW, 2751, Australia*

[2] *School of Plant Biology, The University of Western Australia, 35 Stirling Highway, Crawley (Perth), WA 6009, Australia*

[3] *Department of Biological Sciences, Faculty of Science, Macquarie University, North Ryde, NSW 2109, Australia*

[*] *Corresponding author* (D.Ellsworth@.uws.edu.au)

Running Head: PHOSPHORUS RECYCLING IN PHOTORESPIRATION

ABSTRACT

Leaf photosynthetic CO_2 responses can provide insight into how major nutrients such as phosphorus (P) constrain leaf CO_2-assimilation rates (A_{net}). However, triose-phosphate limitations are rarely employed in the classic photosynthesis model and it is uncertain to what extent these limitations occur in field situations. In contrast to predictions from biochemical theory of photosynthesis, we found consistent evidence in the field of lower A_{net} in high [CO_2] and low [O_2] than at ambient [O_2]. For ten species of trees and shrubs across a range of soil P availability in Australia, none of them showed a positive response of A_{net} at saturating [CO_2] (i.e. A_{max}) to 2 kPa O_2. Three species showed >20% reductions in A_{max} in low [O_2], a phenomenon explained by orthophosphate (P_i) savings during photorespiration. These species, with largest photosynthetic capacity and $P_i > 2$ mmol P m^{-2}, rely the most on additional P_i made available from photorespiration rather than species growing in P-impoverished soils. The results suggest that rarely-used adjustments to a biochemical photosynthesis model are useful for predicting A_{max}, and give insight into the biochemical limitations of photosynthesis rates at a range of leaf P concentrations. Phosphate limitations to photosynthetic capacity are likely more common in the field than previously considered.

INTRODUCTION

The net CO_2-assimilation rate (A_{net}) of C_3 leaves in sunlight comprises three principal processes occurring at the same time: photosynthesis, photorespiration and mitochondrial respiration in the light. A major theoretical advance in the ability to understand and model leaf and canopy CO_2 exchange incorporating elements of all three processes was afforded by the biochemical model of photosynthesis of Farquhar *et al.* (1980), further described in von Caemmerer (2000). This model, originally formulated by Farquhar *et al.* (1980) (here termed the FvCB model) allows for inferences to be made about biochemical limitations to leaf and canopy functioning, overlain by environmental constraints (Long & Bernacchi 2003). The original FvCB model (Farquhar *et al.* 1980) and its subsequent modifications (Sharkey 1985; Sharkey *et al.* 2007; von Caemmerer 2000) successfully predicts photosynthesis under a very wide range of conditions, and has been applied to scales ranging from the chloroplast (von Caemmerer 2013) to forest canopies (Groenendijk *et al.* 2011) and biomes (Bonan *et al.* 2011; Kattge *et al.* 2009). A unique element of the FvCB model is the ability to estimate photorespiratory CO_2 efflux concurrent with photosynthetic CO_2 influx as component processes contributing to the net CO_2-assimilation rate of leaves (Busch 2013; Sage & Sharkey 1987). Both component processes need to be considered to predict net CO_2 assimilation as they occur at the same time, and together have implications for predicting the response of leaf CO_2 assimilation to rising atmospheric CO_2 concentrations, given that elevated [CO_2] both stimulates photosynthesis and suppresses photorespiration (Sharkey 1988; von Caemmerer 2000).

The FvCB biochemical model of photosynthesis has provided a useful context for interpreting many mechanistic aspects of plant function, including how the availability of major nutrients to plant canopies can restrict photosynthetic capacity and net primary productivity (Kattge *et al.* 2009). Analyses of nitrogen (N) limitations to photosynthetic capacity have been based on the fact that a major fraction of leaf N is allocated to the Rubisco enzyme (Evans 1989). The large proportion of leaf N invested in Rubisco and related photosynthetic proteins means that two major parameters of the FBvC model, the maximum carboxylation rate (V_{cmax}) and the capacity for electron transport to support RuBP regeneration (J_{max}), tend to scale linearly with leaf [N] in herbaceous crop species (Archontoulis *et al.* 2012; Evans 1989) and in woody species (Ellsworth *et al.* 2004; Rogers 2014). Such relationships are now used in a number of

56 ecosystem and global-scale models to assess ecosystem productivity of N-limited

57 ecosystems (Piao *et al.* 2013; Rogers 2014; Williams *et al.* 1997; Zaehle *et al.* 2014).

58 However, P limitation of plant productivity is also widespread, with up to one-third of

59 the world's soil orders demonstrating low P availability (Yang & Post 2011). In contrast

60 to N, it is less clear how low leaf P concentration in P-limited systems may affect

61 photosynthetic biochemistry. There are suggestions of both direct and indirect roles of

62 P regulating A_{net} (Domingues *et al.* 2010; Pieters *et al.* 2001; Thomas *et al.* 2006). Hence,

63 a mechanistic representation of P limitations to leaf CO_2 assimilation is rarely

64 implemented in either leaf-to-canopy (Bernacchi *et al.* 2013; Long & Bernacchi 2003;

65 Manter & Kerrigan 2004) or large-scale models (Wang *et al.* 2010), despite the

66 importance of P as a major limiting element across tropical, subtropical and some

67 temperate ecosystems (Aerts & Chapin 2000; Lambers *et al.* 2010; Vitousek *et al.* 2010).

68 Low P supply from soils can affect bulk leaf P concentration and decrease leaf

69 orthophosphate (P_i) pools as well as reduce leaf net CO_2-assimilation rate and other

70 components of photosynthetic biochemistry (Hammond & White 2011; Veneklaas *et al.*

71 2012). Since P-containing molecules such as ATP, NADPH, and sugar-phosphates

72 including ribulose-1,5-bisphosphate (RuBP) have key roles in the Calvin-Benson cycle,

73 lack of sufficient P and P_i would be expected to limit the maximum light- and CO_2-

74 saturated A_{net} (A_{max}) that can be achieved in leaves (Brooks 1986; Loustau *et al.* 1999).

75 Such a decrease in the concentration of these metabolites upon P starvation is typical

76 for plants that are not adapted to P-impoverished soils. Conversely, Proteaceae from

77 severely P-impoverished soils in Australia do not operate at lower leaf P metabolite

78 concentrations at very low soil P availability, but rather replace phospholipids by

79 galactolipids and sulfolipids (Lambers *et al.* 2012) and operate at very low levels of

80 ribosomal RNA and proteins (Sulpice *et al.* 2014). Still, P-limitation might be manifest in

81 limiting RuBP regeneration as the underlying control over A_{max} in leaves (Campbell &

82 Sage 2006; Jacob & Lawlor 1993). Whilst evidence for RuBP regeneration limitation by

83 low P_i exists in laboratory studies (Jacob & Lawlor 1993), the mechanism by which low

84 leaf [P] decreases photosynthetic capacity is not well defined and field evidence of such

85 limitations is still lacking.

86 One approach for quantifying P-limitations to the biochemistry of net CO_2

87 assimilation is by estimating triose-P limitations following theory proposed by Sharkey

88 (1985). The basis of this theory is that RuBP regeneration is adenylate-limited, and a

4

89 release from this limitation is achieved by the release of P_i associated with precursors

90 for sucrose synthesis in the cytosol. Exchange of each released P_i for triose-P produced

91 in the chloroplast allows continued triose-P export to the cytosol (Paul & Foyer 2001;

92 Stitt *et al.* 2010; see A in Fig. 1). An alternative hypothesis is that triose-P limitation is

93 related to how 'closed' the photorespiratory cycle is with regard to the return of

94 glycerate to the chloroplast via photorespiratory glycolate metabolism in the

95 peroxisomes and mitochondria (Harley & Sharkey 1991; Fig. 1, highlighted as B). Short-

96 term low-photorespiratory conditions using low O_2 partial pressure in air (pO_2) can be

97 used as a probe of these biochemical limitation mechanisms to A_{net}. However, whilst

98 triose-P limitations are often mentioned in publications describing the FBvC

99 photosynthesis model, they are rarely parameterised (Bernacchi *et al.* 2013; Manter &

100 Kerrigan 2004), except in very few studies where plants are grown at very low P supply

101 (Bown *et al.* 2009; Domingues *et al.* 2010; Loustau *et al.* 1999).

102   To investigate P limitations to photosynthetic capacity in the field, we sought to

103 determine if these limitations have a role in regulating the biochemical processes

104 underlying leaf A_{net} in the field. We specifically asked *i*) if the standard two-limitation

105 version of the FvCB model (Farquhar *et al.* 1980; Farquhar *et al.* 2001) is adequate to

106 characterise the major parameters controlling photosynthetic capacity for species

107 growing at a range of leaf P and P_i concentrations, *ii*) is there evidence of triose-P

108 limitations to A_{net} using non-photorespiratory gas exchange analysis, and *iii*) are triose-

109 P-utilisation limitations to A_{net} associated with concentrations of bulk leaf P or P_i? Our

110 null hypothesis was that leaf photosynthetic capacity at both normal (ambient pO_2 of 21

111 kPa) and low pO_2 could be described adequately by the two-limitation version of the

112 FvCB model. In this study we used the tool of providing nearly non-photorespiratory

113 conditions by measurements under low pO_2 to gain insight into the processes regulating

114 leaf A_{net}. This was done for Australian sclerophyll plants at a range of leaf P levels in

115 both eastern and south-western Australia, including locations characterised by some of

116 the lowest soil P availabilities on earth (Lambers *et al.* 2010) as well as sites with

117 moderate P availability. In so doing, we sought to resolve whether plants with low leaf P

118 were more likely to show triose-P limitations than those at higher leaf P levels, an idea

119 that is occasionally cited (see Domingues *et al.* 2010; Loustau *et al.* 1999). We chose a

120 set of native species that included species of *Eucalyptus* and *Acacia* and species in the

121 Proteaceae as three groups dominating the Australian continent, and *Liquidambar*

122 *styraciflua* L. which is not native to Australia or similarly low-P soils.

METHODS AND THEORIES

Theory from the Farquhar et al. *(1980) photosynthesis model*

125 Analysis of the instantaneous response of leaf net photosynthesis to brief changes in the

126 CO_2 concentration surrounding leaves underpins the FBvC model parameterisation

127 (Long & Bernacchi 2003; von Caemmerer 2000). According to the standard FvCB model

128 based on the stoichiometry of carbon in photosynthesis and photorespiration (Farquhar

129 *et al.* 1980; von Caemmerer 2000), the net CO_2-assimilation rate of a leaf (A_{net}) can be

130 expressed as

$$\text{A}_{net} = v_c - 0.5 v_o - \text{R}_d = v_c \left(1 - \frac{\Gamma^*}{C_i} \right) - \text{R}_d \qquad (1)$$

132 with v_c and v_o denoting the carboxylation and oxygenation rates of the Rubisco enzyme,

133 R_d representing the rate of mitochondrial respiration in the light, Γ^* representing the

134 CO_2 concentration at which the photorespiratory efflux of CO_2 equals the rate of

135 photosynthetic CO_2 uptake, and C_i indicating the internal CO_2 concentration in the

136 substomatal cavity. As there is also a liquid-phase resistance between the intercellular

137 surfaces and the sites of carboxylation in the thylakoids, this equation is best expressed

138 using C_c, the chloroplastic CO_2 concentration, rather than C_i thus incorporating

139 mesophyll conductance to CO_2 transfer in the liquid phase (Pons *et al.* 2009). Thus,

140 carboxylation rate and hence A_{net} is limited by one of two rates, W_c and W_j (Farquhar *et*

141 *al.* 1980), later revised to include a third rate-limiting process W_t (Sharkey 1985):

$$v_c = \min\{W_c, W_j, W_t\} \qquad (2)$$

143 W_c is the carboxylation-limited rate of net CO_2 assimilation when chloroplastic RuBP is

144 saturating, W_j is the energy transduction for ATP synthesis leading to the subsequent

145 regeneration of ribulose 1,5-bisphosphate (RuBP) in the photosynthetic carbon-

146 reduction cycle, and W_t is the net CO_2-assimilation rate when triose-P pools tie up the

147 available orthophosphate (P_i) for synthesising ATP needed in the photosynthetic carbon

148 reduction or Calvin-Benson cycle (Bernacchi *et al.* 2013; Sharkey *et al.* 2007).

149 When Rubisco activity limits photosynthetic CO_2 assimilation (W_c), A_{net} is given

150 by

151 $$A_{net} = V_{cmax} \frac{C_c - \Gamma^*}{(C_c + K')} - R_d$$ (3)

152 where the half-saturation constant $K' = k_c \left(1 + \frac{O_i}{k_o}\right)$. Here V_{cmax} is the maximum catalytic

153 activity of Rubisco with saturating RuBP, C_c and O_i are the chloroplastic CO_2 and

154 intercellular O_2 gas partial pressures, respectively, and k_c and k_o are the Michaelis-

155 Menten coefficients of Rubisco for CO_2 and O_2 (see Bernacchi *et al.* 2013; Sharkey *et al.*

156 2007). The photosynthetic CO_2-compensation point (Γ^*) is the CO_2 concentration at

157 which the photorespiratory efflux of CO_2 equals the rate of photosynthetic CO_2

158 assimilation. Given that the Rubisco enzyme is characterised by relatively conservative

159 kinetic properties among different lineages of higher C_3 plant species, k_c, k_o and Γ^* can

160 be assumed as relatively invariant among species (Bernacchi *et al.* 2001; but see Galmés

161 *et al.* 2005; Walker *et al.* 2013). In the classic version of the FvCB model, when C_c is

162 close to saturation for photosynthesis such that RuBP regeneration limits

163 photosynthesis (W_j is limiting), A_{net} is given by

164 $$A_{net} = J_{max} \frac{C_c - \Gamma^*}{(4C_c + 8\Gamma^*)} - R_d$$ (4)

165 where J_{max} is the maximum rate of electron transport at saturating quantum flux density

166 to provide energy for RuBP regeneration in the PCR cycle. Most frequently, the

167 parameters V_{cmax} and J_{max} are investigated as the major components of the

168 photosynthesis model (Cernusak *et al.* 2011; Kattge *et al.* 2009; Rogers 2014; Walker *et*

169 *al.* 2014) assuming two major biochemical limitations to A_{net}. However, as originally

170 stated, the FvCB photosynthesis model has no explicit dependence of J_{max} on O_2 partial

171 pressure except Γ^* in Eqn 4. The Γ^* term is a function of the *in vivo* substrate specificity

172 factor for the Rubisco enzyme ($S_{c/o}$), given as:

173 $$\Gamma^* = \frac{0.5 \cdot O}{S_{c/o}}$$ (5)

174 Where $S_{c/o}$ is here considered ≈ 92 mol mol^{-1} at 25°C, within the range reported for C_3

175 woody species (Galmés *et al.* 2005). The original version of the FvCB photosynthesis

176 model produces predictions of the A_{net}-C_c response at normal air pO_2 (21 kPa, hereafter

177 referred to as normal pO_2) and low-photorespiratory pO_2 that are illustrated in Fig. 2

178 (see also von Caemmerer 2000).

179

180

FvCB photosynthesis model with triose-phosphate limitation included

Two modifications of the original FvCB model were subsequently proposed to account for the behaviour of A_{net} measured at high CO_2 partial pressures and with suppression of photorespiration at experimentally reduced O_2 partial pressures. These changes to the model accounted for two physiological states that have been observed both at high CO_2 partial pressures: *i*) O_2 insensitivity of A_{net} at high pCO_2, and *ii*) reverse O_2 sensitivity of A_{net}. In the first version, synthesis of sucrose from triose-phosphates was thought to make a contribution to P_i recycling for photophosphorylation since the triose-P transporter exchanges triose-P for P_i. For the situation when the rate at which triose phosphates are utilised (T_p) in the synthesis of carbohydrates limits A_{net} (W_t in Eqn 2), Sharkey (1985) proposed that

$$A_{net} = 3 \cdot T_p - R_d \tag{6}$$

As there is no term dependent on pO_2 in Eqn 6, there is no explicit sensitivity to low pO_2 in this variant of the model. It was found that this model version might not always account for leaf gas exchange behaviour in low pO_2 (Harley & Sharkey 1991; Sage & Sharkey 1987), promoting an updated version of the model formulation.

In this updated version, Harley & Sharkey (1991) further proposed consideration of the pO_2 sensitivity of light- and CO_2-saturated net CO_2-assimilation capacity (A_{max}) through an 'open' photorespiratory C cycle. This version of the FvCB model has a pO_2 sensitivity that originates indirectly from ATP consumed with metabolism of the photorespiratory product, glycolate, in the chloroplast (α_g) (Fig. 1, B) as given by

$$A_P = \frac{\left(C_c - \Gamma^*\right) \cdot 3 T_p}{C_c - \left(1 + 3 \cdot \alpha_g\right) \cdot \Gamma^*} - R_d \tag{7}$$

The parameter α_g is multiplied by three to reflect the stoichiometry of P_i consumption in oxygenation (von Caemmerer 2000; note the correct version of the equation here), and varies as a fraction between 0 and 1 depending on whether all glycolate returns to the chloroplast (a 'closed' photorespiratory cycle where C is maximally conserved, in which case Eqn 7 simplifies to Eqn 6), the return is partial, or glycolate is entirely diverted to amino acid synthesis leaving none to return (Harley & Sharkey 1991).

More than 20 years after it was proposed, this third term of the model (Eqns 6 and 7) is rarely considered in photosynthesis model fits to data (von Caemmerer 2013) and most often ignored (Kattge *et al.* 2009; Manter & Kerrigan 2004; Walker *et al.*

213 2014). This is due in part to a lack of appropriate measurements (Long & Bernacchi

214 2003; von Caemmerer 2000) and because the evidence supporting its importance in

215 leaves with low P concentration has been equivocal (Domingues $et\ al.$ 2010). Moreover,

216 T_p has almost never been parameterised in field situations, so it remains unclear if this

217 term needs to be considered in modelling limitations to photosynthetic CO_2 assimilation

218 (Bernacchi $et\ al.$ 2013). If T_p can largely be ignored, we expect a stimulation of A_{net} by

219 low pO_2 in all parts of the CO_2-response curve as per Figure 2. Our field measurements

220 of plants at high and low leaf P status aimed to understand if the mechanistic

221 hypotheses of triose-P limitations to photosynthesis portrayed in Eqns 6 and 7 are

222 consistent with field data, and if these revisions can reflect the role of P availability for

223 regulating A_{net}. If there is an association between plant P status and T_p, then

224 incorporation of this parameter into models may improve the predictability of A_{net},

225 especially where rising atmospheric CO_2 concentration and low soil P availability are

226 concerned.

227

228 *Research sites and plant material*

229 The research was conducted on trees and shrubs growing at five different sites in

230 eastern and south-western Australia (Table 1), with different soil substrates and parent

231 materials resulting in different leaf P content in their characteristic species. Sites were

232 chosen based on known aspects of their mineralogy and previous studies on leaf

233 nutrients (e.g., Lambers $et\ al.$ 2012) so that they would provide a range in leaf total P

234 and P_i fraction and thus presumably represent a range in P_i limitations to A_{net}. Four of

235 the five sites were infertile and low in P availability, with the fifth site on a richer soil.

236 The Davies Park site is located at 390 m above sea level (a.s.l.) in the Blue Mountains in

237 eastern Australia on thin soils overlaying Hawkesbury sandstone, a Triassic

238 sedimentary quartzose sandstone formed over 200 Mya. The soils derived from the

239 Hawkesbury sandstone in the Blue Mountains are shallow (5-20 cm depth) and very

240 infertile with low P availability. The Hawkesbury Forest Experiment and adjacent

241 Hawkesbury campus and EucFACE sites are all located at 30 m a.s.l. within 1 km of one

242 another on Clarendon loamy sand, a deep, alluvial soil formed in the late Pleistocene by

243 meanders of the Hawkesbury river around 1.5 Mya. The soil is a low-fertility loamy

244 sand, with soil surface total P concentrations of 60 mg kg^{-1} soil in the upper 15 cm

245 (Ellsworth $et\ al$., unpubl. data), but a large fraction of this P is sorbed onto

246 aluminosilicates and ferro-manganesian silicates (Holford 1997). One of the plantations

247 at this site (*Liquidambar styraciflua* L.) was horticulturally managed and had

248 periodically-amended soil P. The Lesueur National Park site is described in detail in

249 (Lambers *et al.* 2012). This site is located near Jurien Bay, WA and occurs at 80 m a.s.l.

250 on shallow colluvial sand and lateritic gravel over weathered sandstone from the late

251 Jurassic Yarragadee Formation (150-185 million years old; Griffin & Burbidge 1990).

252 The sandy soil at this site is extremely low in P, with a total P of 9.5 mg kg^{-1} soil in the

253 upper 30 cm (Lambers *et al.* 2012). The fifth site, Illawarra Fly in Robertson NSW, is a

254 fertile site on young soils. This site occurs at 710 m a.s.l. elevation on soils of the

255 Illawarra escarpment that are brown clay loams underlain by Paleocene/Pliocene

256 basalt. These basaltic soils in the area are relatively fertile with total P of 1010 mg kg^{-1}

257 soil and frequently managed for farming, though this particular site was in a never-

258 farmed parcel of mature remnant wet sclerophyll forest. Since sites differed in

259 elevation, amounts of gases such as CO_2 and O_2 are reported as partial pressures (e.g.,

260 pO_2) rather than mole fractions.

261   Whilst the focus was on measuring species of *Eucalyptus* as native dominants in

262 the study regions, non-Myrtaceous species were also included (*Banksia* spp. and

263 *Persoonia levis*, all Proteaceae, and *Acacia oblongifolia*). An exotic deciduous plantation

264 tree, *Liquidambar styraciflua*, was also included in the study so that inferences would

265 not be strictly limited to native Australian sclerophyll species, which are considered to

266 be well-adapted to low soil P (Beadle 1966).

267

268 *CO_2-exchange measurements*

269 In this study, photosynthetic CO_2-response curves (A_{net} - C_i response curves) were made

270 *in situ* on ten species of trees and shrubs at five sites in Australia (Table 1) using a

271 portable photosynthesis system (LiCor 6400XT, Licor Inc., Nebraska USA) with 6 cm^2

272 chamber. All measurements were made on attached, intact leaves at the top of the

273 crown or the outer shell of the crown when open-grown which meant accessing leaves

274 from 1 m up to 25 m high (Table 1). For tall species, access to the upper parts of the tree

275 crowns was achieved by three different means: an articulated boom lift (Snorkel

276 MHP13/35 Trailer Mounted Lift, Snorkel Ltd., Meadowbrook, Qld, Australia) used at the

277 Hawkesbury site in Richmond NSW, a set of 36 m tall construction cranes (Jaso crane J-

278 4010, Jaso S.L., Idiazabal, Spain) at the nearby EucFACE site in Richmond NSW, and a

279   custom-built steel-alloy canopy walkway going up from ground level to 30 m height

280   ('Illawarra fly') at Robertson, NSW. Canopy access was not necessary at the Lesueur

281   National Park site or at Davies Park, as trees and shrubs were open-grown in each of the

282   sclerophyll woodlands, and unshaded leaves at the outside of the crown could be

283   readily measured.

284   We made field measurements of the instantaneous response of leaf net CO_2

285   assimilation to changes in the external CO_2 concentration according to Ellsworth *et al.*

286   (2004), using standard coefficients recommended in Sharkey *et al.* (2007) when fitting

287   the FvCB model (see below). A_{net}-C_c response measurements on all species were made

288   during the growing season in summer and autumn at seasonal temperatures and during

289   periods of recent rainfall to reduce complications due to drought. Previous–year's

290   leaves were measured rather than newly-emerged leaves to ensure that leaves were

291   operating at their full photosynthetic capacity (see Denton *et al.* 2007; Lambers *et al.*

292   2012). The A_{net} measurements were made in morning hours on sunny days so as to

293   avoid stomatal closure and mid-day depression of A_{net}.

294   The A_{net}-C_c response curves were started by maintaining the CO_2 concentration

295   (C_a) in the gas exchange chamber at ambient CO_2 partial pressure (~38-39 Pa in this

296   study) until gas-exchange rates were stable, then recording measurements. Steps for the

297   curves were generated by decreasing C_a to near the compensation point (5 Pa), and then

298   increasing C_a stepwise across 8-9 steps (Ellsworth *et al.* 2012) at a constant

299   photosynthetic photon flux density of 1800 µmol m^{-2} s^{-1}, 50-70% relative humidity, and

300   a controlled leaf temperature (between 26 and 28°C, depending on species). The mean

301   leaf-air vapour pressure deficit of the measurements was 1.5 ± 0.1 kPa. At each C_a step,

302   we recorded A_{net}, g_s, C_i and associated variables when stability was reached. Upon

303   completion of measurements, leaves were placed on ice or liquid nitrogen until ready

304   for further analysis. In the lab, leaf thickness was measured at five points on the leaf

305   lamina using digital callipers (Mitutoyo Corp, Kawasaki, Kanagawa, Japan).

306   In the process of these A_{net}-C_c response measurements, at four or five of the C_a

307   steps, we ensured that parallel measurements at ambient oxygen (21 kPa) and low-

308   photorespiratory oxygen (2 kPa) were made. Low pO_2 inside the gas exchange chamber

309   was generated by routing a low-O_2 tank gas (Air Liquide Australia Ltd., Melbourne,

310   Australia) to the leaf chamber, supplied at the same slight over-pressure as for ambient

311   air as described by Li-Cor (Li-Cor 2008) and with the excess flow to the Li-6400 pump

312   monitored with a rotameter. A Teflon T-valve was toggled between ambient air with 21

313   kPa pO_2 and 2 kPa tank gas at the appropriate C_a steps (up to five C_a steps including at

314   saturation). These steps were chosen in order to minimally define the initial rise to a

315   maximum and the maximum asymptote for the A_{net}-C_c curve at low pO_2, given that the

316   shape of these curves has long been known (Laing *et al.* 1974; von Caemmerer 2000).

317   The flow excess was maintained around 0.3 L min^{-1}. Measurements of A_{net} in 2 kPa pO_2

318   were completely reversible as described in Laing *et al.* (1974)(see Supporting

319   Information, Fig. S1).

320

321   *Calculations of O_2 corrections and mesophyll conductance to CO_2*

322   We used three corrections for changes in pO_2 in the carrier-gas in the LI-6400XT

323   photosynthesis system that originated from the change in density due to different gas

324   concentrations. The corrections employed were: i) increased air-flow rate through the

325   CO_2-injector system due to reduced air viscosity with decreased pO_2 , ii) band

326   broadening of CO_2 infrared absorption (Burch *et al.* 1962) incorporated into the

327   standard Li-6400 software, and iii) band broadening of water vapour infrared

328   absorption (Bunce 2002).

329   Given theoretical issues raised by Gu & Sun (2014) concerning the dependence

330   of mesophyll conductance to CO_2 (g_m) on C_i, we assumed a constant g_m for different C_i

331   steps in the response-curve data. Mesophyll conductance was either measured or

332   estimated for each species for calculations of C_c. For three species amongst those in

333   Table 1 ranging in A_{net} from highest and lowest, we measured instantaneous g_m with

334   online carbon-isotope discrimination using tunable diode laser absorption spectroscopy

335   (TDLAS; Campbell Scientific TGA100A, Logan, UT, USA). Our g_m calculations follow

336   Tazoe *et al.* (2011) with further description in Crous *et al.* (2013). We then estimated

337   mean g_m of all the species using a relationship for g_m as a function of g_s from our

338   measurements (g_m = -0.04 + 1.34*g_s, r^2 = 0.54; Supporting Information Fig. S2). In a

339   review of available data, g_m usually scaled with g_s especially amongst well-watered

340   plants (Flexas *et al.* 2012). After incorporating g_m, we derived biochemical model

341   parameters using the A_{net}-C_c data.

342   Photosynthetic parameter fits were done in R (Team 2014) using kinetic

343   coefficients in Sharkey *et al.* (2007) to standardise the fits across species, but using Γ*

344   and its temperature dependence specifically measured for *Eucalyptus* (Crous *et al.*

345   2013). We fit V_{cmax}, J_{max} and T_p piece-wise using specified ranges of conditions where

346   each parameter was judged to limit A_{net} following guidelines in Sharkey *et al.* (2007)

347   with the nonlinear solutions generated using the 'optim' package in R. T_p was fit for A_{net}

348   when $C_c > 40$ Pa and pO_2 of 2 kPa. As a more robust fitting approach with fewer

349   assumptions, we also pooled data for all leaves within a species and simultaneously

350   solved for species-level V_{cmax}, J_{max} and T_p at both pO_2 levels using the 'nls' package in R.

351   Across species, the two sets of solutions agreed well with one another, since slopes for

352   each parameter were close to unity (slopes of 0.981, 0.966 and 0.840 for V_{cmax}, J_{max} and

353   T_p, respectively, estimated for piecewise compared with simultaneously-solved). V_{omax},

354   the maximum velocity of oxygenase activity, was fit to the data from both pO_2 levels for

355   low C_c where oxygenase activity of Rubisco is considered limiting, following equations

356   in Farquhar *et al.* (1980).

357

358   *Leaf chemical analyses*

359   After measurements, leaves were immediately placed on ice and transported to the

360   laboratory, where thickness and area were measured on a subsample, whilst the

361   remainder was frozen and subsequently dried to a constant mass at 70 °C. The leaf

362   lamina dry mass per unit area (M_a) was calculated from the ratio of dry mass to fresh

363   area. The dried sample was ground finely in a ball mill, and used for analyses of total N

364   concentration, total P concentration, inorganic P (P_i) concentration, and starch and

365   soluble sugar concentrations. Leaf N concentration was analysed by elemental analysis

366   after combustion using a CHN elemental analyser (TruSpec micro, LECO Corp., St.

367   Joseph, MI, USA; or FLASH EA 1112 Series CHN analyser, Thermo-Finnigan, Waltham,

368   MA USA). Leaf total P concentrations were measured after digesting dried leaf tissue

369   with concentrated sulfuric acid (H_2SO_4) and hydrogen peroxide (H_2O_2) in a microwave

370   digester apparatus (Berghof speedwave four, Berghof Products GmbH, Eningen,

371   Germany). The solutions containing total P or the P_i fraction were analysed

372   colourimetrically at 880 nm (AQ2, SEAL Analytical, Ltd., Milwaukee, WI USA) after a

373   standard molybdate reaction (Close & Beadle 2004). Analyses of N and P concentrations

374   used international standards run blind alongside the samples, and are expressed as N

375   and P content (mmol m^{-2}) in this manuscript due to differences in leaf thickness

376   amongst the species (Table 1). Bulk leaf P_i was determined by extracting samples in 0.3

377   M TCA at 4 °C before cold centrifuging at 9224 × g (10,000 rpm) for 5 min and collecting

378 the filtrate (Close & Beadle 2004). The P_i concentrations in the samples were

379 determined against standards made with KH_2PO_4 in serial dilution.

380 **RESULTS**

381

382 The set of species used in this study ranged two-fold in their leaf thickness, and nearly

383 ten-fold in their leaf P content (Table 1). A_{net} varied more than two-fold, between 10 and

384 26 µmol m^{-2} s^{-1} among the species when measured at C_i between 27-28 Pa. As a

385 stoichiometric index of P versus N limitation, six of the ten species studied had N:P

386 ratios > 20, while *E. fastigata* and *L. styraciflua*, both from moderately-fertile conditions,

387 had N:P of 10-13 (see Supporting Information, Table S1).

388   Biochemical modelling from A_{net} - C_c response curves at both 21 and 2 kPa pO_2

389 using the classic FvCB model would suggest a slightly higher A_{net} asymptote at high C_c

390 and low pO_2 (i.e. similar A_{max} at ambient and low pO_2) due to the lower Γ^* as per Eqn 5

391 above (Fig. 2). Thus, a stimulation of A_{net} by low pO_2 was expected both in the

392 carboxylation-limited region of the CO_2-response curve and, though smaller, also in the

393 RuBP-regeneration-limited region or where A_{net} is saturated with respect to C_a.

394 Consistent with this, there was an average of 23% stimulation in A_{net} at ambient CO_2

395 under low-photorespiratory conditions using 2 kPa pO_2 in the carboxylation-limited

396 region of the A_{net} - C_c response curve (Fig. 3 and data not shown). However, in contrast

397 to theoretical expectations, none of the ten species measured showed the expected

398 small A_{net} stimulation in the RuBP-regeneration-limited region in 2 kPa pO_2 compared

399 with A_{net} in normal pO_2. Rather, species either showed similar A_{max} values as asymptotes

400 to the A_{net} - C_c response in 2 kPa pO_2 compared with 21 kPa pO_2 (Fig. 3A,B), or a

401 dramatic reverse response for the A_{max} in 2 versus 21 kPa pO_2 (Fig. 3C,D), with about a

402 20% reduction in A_{max} at 2 kPa pO_2 compared with normal pO_2. The cross-over between

403 curves at normal and low pO_2 occurred at C_i values as low as 28 Pa, up to 40 Pa

404 depending on species. In low pO_2 there was also a sharp transition between Rubisco-

405 limited photosynthesis at low C_c and RuBP-regeneration and T_p limited photosynthesis

406 compared to normal pO_2 (Fig. 3). For our study species, the difference in A_{max} between

407 normal and low pO_2 was between 2 and 14 µmol m^{-2} s^{-1} (average of 5.8 µmol m^{-2} s^{-1}),

408 with low pO_2 values consistently lower. This was significantly different from zero for all

409 species, even for *B. attenuata* (P=0.017 in a one-tailed t-test) and *P. levis* (P = 0.01), both

14

of which had rather small mean differences in asymptotic A_{net} between normal and low pO2 of about 2 µmol m^{-2} s^{-1} (Fig. 3A,B). This result establishes that there was a reverse sensitivity of A_{net} to the reduction in pO2 at high C_c across the range of species measured in the field. Given that this reverse sensitivity in low pO2 conditions was significant in all species, we considered it valid to use the model of Harley & Sharkey (1991) to estimate the P limitation component of the biochemical model, rather than the simpler model of Sharkey (1985) that has been recommended to standardise model fitting.

Estimates of V_{cmax} from independent gas-exchange measurements at either pO2 level were similar (Fig. 4A). However, we could not recover the same A_{max} in different pO2 levels using the traditional two-parameter FvCB photosynthesis model (Fig. 4B). The A_{max} estimated in low pO2 was lower than expected based on A_{max} in normal pO2 (under the 1:1 line in Fig. 4B). The largest A_{max} reductions in low pO2 were in species with high A_{max} at normal pO2, such as *E. fastigata* and *L. styraciflua* (average of 8 and 12 µmol m^{-2} s^{-1} lower, respectively). This was further evidence that an additional parameter to the FvCB photosynthesis model was needed to fit photosynthesis to our field measurements. The difference in modelled A_{max} using the traditional FvCB model to the A_{max} predicted by the model revision proposed by Harley & Sharkey (1991) was largest for species with high A_{max} in normal air (21 kPa pO2; Fig. 4C). Fitting the T_p parameter using Eqn 7 proposed by Harley & Sharkey (1991) to the data, we were able to recover the A_{max} that we had measured in low pO2 (Fig. 4D). Taken together, all species showed a reduced A_{max} at low pO2, with the largest reductions occurring in species with the highest A_{max}. These reductions were recovered once the T_p parameter (Eqn 7) was employed in the model fits.

The difference in A_{max} for the model without T_p considered versus the model with T_p considered was positively correlated with leaf P_i content up to a threshold of about 2 mmol P_i m^{-2} (r^2 = 0.4, P < 0.0001), beyond which there was no apparent relationship (Fig. 5). There was a similar but weaker relationship (r^2 = 0.2) for total T_p below a threshold of ~10 mmol P m^{-2} (not shown). T_p was itself only very weakly correlated with leaf P_i content up to a threshold of 2 mmol P_i m^{-2} (r^2 = 0.10, P < 0.01; data not shown). Six species (*A. oblongifolia*, *B. attenuata*, *B. serrata*, *E. todtiana*, *E. tereticornis* and *P. levis*) all had leaf P_i contents in the linear region, where the magnitude of suppression of CO2-saturated photosynthesis by low pO2 varied strongly with P_i. *E. fastigata* and *L. styraciflua* both had high leaf P_i contents and high A_{max} differences,

443   falling in the saturating region of Fig. 5. The amount of total leaf P present as P_i averaged

444   $30 \pm 2\%$ (mean ± s.e.) among the species in our study. *Liquidambar styraciflua* had the

445   highest free P_i in leaves, at $46 \pm 4\%$ of total leaf P concentration. *B. attenuata*, *B. serrata*

446   and *P. levis* had the lowest total leaf P concentrations (around 0.35 mg P g^{-1}; Table S1),

447   but similar P_i fractions as the species average above.

448   For the set of ten species across a range in soils and P supply levels, the

449   individual photosynthetic model components V_{cmax}, J_{max}, and T_p were all correlated with

450   leaf chemical traits, though correlations with total leaf P_{area} were strongest (Table 2, Fig.

451   6). The three species from Davies Park in the Blue Mountains of NSW had the lowest leaf

452   P_{area} closely followed by those from Lesueur National Park in Western Australia. The

453   strongest relationship between the biochemical components of leaf photosynthetic

454   capacity and leaf chemistry was between J_{max} and leaf P_{area} (R^2 = 0.66, Fig. 6c). Bivariate

455   relationships between photosynthetic model components and leaf N_{area} were not

456   significant ($P > 0.10$, Table 2), nor was A_{max} associated with leaf N_{area} across the set of

457   species. There were no significant relationships between any of these traits and M_a.

458   V_{omax} was not significantly correlated with N_{area}, and was only marginally significantly

459   correlated with P_{area} ($P = 0.052$; Table 2 and Fig. 6b). V_{omax} fit to data at both

460   measurement pO_2 levels was significantly correlated with V_{cmax} fit to measurements at

461   both pO_2 ($P = 0.0052$; not shown) with a slope of 0.17 and a significant y-intercept.

462   **DISCUSSION**

463

464   Reductions in A_{max} during exposure to low pO_2 have been documented for over 50 years

465   (Joliffe & Tregunna 1968), but have rarely been measured in the field. Despite

466   suppression of photorespiration by low pO_2 at the current atmospheric C_a (Fig. 2), we

467   have shown that A_{net} at high C_i and low pO_2 is reduced, rather than higher as would be

468   expected from theory based on the biochemical regulation of photosynthesis (Farquhar

469   *et al.* 1980; Laing *et al.* 1974; von Caemmerer & Farquhar 1981). All ten tree and shrub

470   species studied at a range of Australian sites showed this response to varying degrees,

471   at moderate summertime temperatures (Fig. 4). According to the Harley & Sharkey

472   (1991) theoretical model, when leaves operate at near-saturating C_i, photorespiratory

473   glycerate may not completely re-enter the PCR cycle, so that P_i released by phospho-

474   glycolate phosphatase in the chloroplast, that would normally have been used by the

475 glycerate kinase reaction upon photorespiratory C return to the chloroplast, is instead

476 available in the stroma for RuBP regeneration (Fig. 1, B). Under low-photorespiratory

477 conditions, this additional source of P_i becomes unavailable, resulting in slower RuBP

478 regeneration and lower A_{max} at low pO_2 than at normal pO_2. Modelling using the

479 equation for T_p in Harley & Sharkey (1991) gives A_{max} results that are broadly consistent

480 with our data (Fig. 4). While limitations to photosynthesis by triose-P utilisation are

481 considered to be uncommon and are often ignored in photosynthetic model-fitting, our

482 field measurements under low-photorespiratory conditions show that T_p can be limiting

483 A_{max} in a wide range of woody species.

484 　　　　An alternative hypothesis for T_p limitations to A_{max} suggests that excessive

485 synthesis of triose-P to be exported from the chloroplast increases recycling of P_i

486 entering chloroplasts, with higher stromal P_i leading to the accumulation of 3PGA and

487 decreasing phosphoglucoisomerase activity and suppressing starch synthesis (Sharkey

488 1985; Stitt *et al.* 2010; Fig. 1, A). While simpler in concept and in formulation (Eqn 6),

489 the T_p limitation emerging from conservative C cycling back to the chloroplast cannot

490 explain what we found here, because it describes pO_2-insensitive photosynthesis, whilst

491 we found a strong reverse sensitivity of A_{max} to low pO_2 which is only predicted by the

492 Harley & Sharkey (1991) model of T_p limitation. Previous treatments using the Sharkey

493 (1985) formulation did not conduct measurements at low pO_2 at a range of C_a levels,

494 and thus have not been able to distinguish between pO_2-insensitive and reverse-

495 sensitive photosynthesis.

496 　　　　On the basis of the Harley & Sharkey (1991) model, our data provide strong

497 evidence that not only is photorespiration a source of amino acids through NH_3 release

498 in glycine metabolism (Wingler *et al.* 2000), but also that glycolate diversion from re-

499 entry into the chloroplast during photorespiration simultaneously frees stromal P_i to

500 permit enhanced photophosphorylation and RuBP regeneration, thus permitting high

501 A_{max}. Measurements of this phenomenon on a much broader set of C_3 plant species is

502 needed to understand the generality of this phenomenon, but the set of species we

503 studied represents a range of phylogenies and includes species with different affinities

504 for growing on low-P sites. All these species showed significant decreases in A_{max}

505 measured during transient non-photorespiratory conditions. The decreases in A_{max} in

506 low pO_2 for *L. styraciflua*, *E. fastigata* and *E. dunnii* were all greater than 5 μmol m^{-2} s^{-1}

507 and as high as 12 μmol m^{-2} s^{-1} (in *E. fastigata*), and thus were much larger than those of

508 the order of 2 µmol m^{-2} s^{-1} shown for soybean in Harley & Sharkey (1991). Therefore,

509 we suggest that this phenomenon may be common amongst a number of plant genera,

510 and potentially across a significant geographic expanse. There is a need for broader

511 consideration of this mechanism among species, as currently T_p limitations to A_{max} are

512 ascribed to the parameter J_{max} in a large number of studies (for example, Kattge *et al.*

513 2009; Manter & Kerrigan 2004; Walker *et al.* 2014). We also suggest that the

514 mechanism proposed by Harley & Sharkey (1991) is more properly called phosphate

515 limitation rather than triose-P limitation, since triose-P is not necessarily integral to the

516 proposed mechanism (see Fig. 1, B). Nevertheless, we have retained the terminology of

517 Harley & Sharkey (1991) in fitting Eqn 7, but suggest that T_p can be more broadly

518 considered as phosphate limitation to A_{net}.

519   Internal recycling of P_i in cells is important for the balanced production of ATP

520 and regeneration of RuBP as essential requirements for high CO_2-assimilation rates.

521 While a source for P_i for photophosphorylation to regenerate RuBP as depicted in Fig. 1

522 (see B in Fig. 1) could be a valuable mechanism for sustaining A_{net} at high C_i in plants in

523 conditions with limiting soil P, our measurements do not suggest this occurs at the

524 extremely low P levels characterising both the Lesueur National Park and Davies Park

525 sites. Among the ten woody species we measured including some on infertile sites with

526 low soil P-availabilities, plants with low leaf P concentrations (total leaf P < 400 µg g^{-1},

527 for instance) also had slow rates of photorespiration and an apparent high fractional

528 return of photorespiratory glycerate to the chloroplast, resulting in a relatively small

529 inhibition of A_{max} in low pO_2 and high C_i (Fig. 3a,b). However, our findings are consistent

530 with the previously-overlooked mechanism of glycerate sequestration during

531 photorespiration may in fact be common in a number of woody species. This

532 mechanism operates at high C_i (but to C_i as low as 28 Pa depending on species; Fig. 3)

533 which means that it is relevant for a substantial fraction of canopy leaves maintained in

534 shade where RuBP regeneration and triose-P supplies may limit A_{net}. It may also be

535 relevant in elevated atmospheric CO_2 concentrations (Campbell & Sage 2006) with a

536 role in increasing the degree of cellular P_i-deficiency with decreased photorespiration,

537 expected as C_a increases in the future. The mechanism hypothesised by Harley &

538 Sharkey (1991) and supported by our data is not yet considered in physiologically-

539 based models used to project plant CO_2 assimilation behaviour into the future (Wang *et*

540 *al.* 2010). Our identification of this mechanism in the field opens an important new area

541 of research relevant to expected future conditions including elevated $[CO_2]$, and further

542 field measurements of this sort are crucial to help resolve the range of ecological

543 contexts where P_i regulation over A_{max} may be most important.

544   The hypothesised mechanism for net P_i release in the chloroplast described by

545 Eqn 7 and shown in Fig. 1 requires glycolate exported from the chloroplast to be

546 sequestered, metabolised or exported from the cell, rather than being converted into

547 glycerate for re-entry into the chloroplast. What are the possible mechanisms for this C

548 "diversion" rather than conservation by chloroplast re-entry? Harley & Sharkey (1991)

549 cited ^{14}C labelling evidence to suggest photorespiratory C export by the vascular system

550 to other parts of the plant (Wingler *et al.* 2000), and at least 12% of the amino acid

551 composition of phloem in *Eucalyptus* comprises serine and glycine (Merchant *et al.*

552 2010), demonstrating that this export is plausible. There are other plausible fates for

553 this C that may also be important (Reumann & Weber 2006). Glycolate and glyoxylate

554 products of photorespiration (Fig. 1; Wingler *et al.* 2000) can be oxidised by glycolate

555 oxidase in the peroxisome to form oxalic acid, which is stored in vacuoles or

556 metabolised to calcium oxalate crystals, common in a wide range of plants (Franceschi

557 & Nakata 2005) and documented for both *Eucalyptus* and *Acacia* (Brown *et al.* 2013).

558 Alternatively, oxalate might be metabolised again (Havrir 1984) and allow glycerate re-

559 entry into the chloroplast when the requirement for P_i is less. Glycine participates in the

560 early steps of porphyrin synthesis in the mitochondria as part of chlorophyll assembly

561 (Beale 1978) as well as in the synthesis of glutathione, which is involved in stress

562 protection (Wingler et al. 2000). Whilst the ultimate fate of photorespiratory glycolate

563 may vary amongst different plant species, evidence of multiple mechanisms driving a

564 lack of C return to the chloroplast after photorespiratory metabolism provides support

565 for the sequestration of glycolate or its products after photorespiration, a key part of the

566 hypothesised mechanism of Harley & Sharkey (1991).

567   Some implications of the incomplete photorespiratory glycerate re-entry and

568 subsequent extra available P_i (see B in Fig. 1) are that species with low photorespiration

569 such as Proteaceae (*B. attenuata*, *B. serrata*, *P. levis*; see Supporting Information, Table

570 S1) would have a low flux rate of chloroplastic P_i made available by this mechanism

571 compared with species with higher photorespiration. Some Proteaceae species also

572 allocate more P to their mesophyll cells rather than their epidermal cells (Lambers *et al.*

573 2015) , compared with other dicots that have relatively high P levels in epidermal cells

574   (Conn & Gilliham 2010). Indeed, five species in our study (*B. attenuata*, *B. serrata*, *E.*
575   *todtiana*, *E. tereticornis* and *P. levis*) all have a leaf P_i content where the magnitude of
576   suppression of A_{max} by low pO_2 varies strongly with P_i ($P_i < 2$ mmol m^{-2}, Fig. 5). This
577   suggests that at low leaf P contents, these species must rely on existing stromal P_i pools,
578   rather than those saved by the lack of glycerate re-entry during photorespiration at high
579   C_i. Lambers *et al.* (2012) showed that photosynthetic cells of mature *Banksia* leaves
580   extensively replace phospholipids by lipids that do not contain P, i.e. galactolipids and
581   sulfolipids, which reduces their demand for P_i for lipid synthesis and hence increases P_i
582   available for participation in photosynthetic carbon metabolism. Moreover, these
583   species also operate at very low levels of ribosomal RNA (Sulpice *et al.* 2014), which is a
584   major fraction of leaf P (Veneklaas *et al.* 2012). Mechanisms for internal P conservation
585   such as these may obviate the need for P contributed from the lack of photorespiratory
586   glycerate re-entry mechanism in P-impoverished ecosystems.

587   Amongst the species we measured, *L. styraciflua*, *E. saligna* and *E. fastigata*
588   showed the fastest RuBP regeneration rates (i.e. high J_{max}), the highest leaf P_i contents,
589   and also showed the largest decreases in A_{max} at low pO_2. Why do these fast-metabolism
590   plants show an apparently large T_p limitation of A_{max}, when they also have high P_i? The
591   bulk leaf P_i measurements are indicative but inconclusive as only the chloroplastic P_i
592   fraction is relevant to the hypothesised mechanism. The reverse sensitivity to pO_2 at
593   high C_c can occur in species with high photosynthetic activity where the requirement for
594   P_i for ATP synthesis is balanced against the need to maintain low P_i for starch and
595   sucrose synthesis (Sharkey & Vassey 1989). With rapid triose-P production in
596   photosynthesis exceeding the capacity to use triose-P in such species, low pO_2 would
597   decrease photorespiration and reduce P_i from dephosphorylation of phosphoglycolate
598   as well as greatly reduce carbon leaving the Calvin-Benson cycle by serine and/or
599   glycine export. It is not clear yet if these two mechanisms are mutually exclusive, but
600   they are consistent with the data in Figure 5.

601   There is an additional possibility that the T_p limitation of species with high A_{max}
602   may occur due to the high P requirements in such species for ribosomal RNA (rRNA),
603   which is needed to support rapid rates of protein synthesis and growth (Matzek &
604   Vitousek 2009; Niklas *et al.* 2005). The P contained in RNA, particularly rRNA, is a
605   significant fraction of the total non-vacuolar P in leaves (Raven 2012). Hence, if high P
606   costs of rRNA for protein turnover are necessary to support rapid photosynthesis in

607 mature leaves as suggested by Veneklaas *et al.* (2012) and others (Matzek & Vitousek

608 2009), then this protein synthesis may be achieved from two concurrent

609 photorespiratory products. Amino acids are generated from photorespiratory ammonia

610 (NH_3) release in glycine decarboxylation (Wingler *et al.* 2000), and the lack of

611 photorespiratory glycerate re-entering the chloroplast frees chloroplastic ATP for

612 enhancing RuBP regeneration and increasing A_{max}, while also freeing P_i for P-rich

613 ribosomes to generate proteins in the stroma (Fig. 1). How much glycine or serine is

614 directed away from the photorespiratory pathway and chloroplast re-entry and rather

615 used for protein biosynthesis is unclear. However, the release of N from

616 photorespiration may be as large as from nitrate reduction (Wingler *et al.* 2000), and

617 hence the release of ATP for RuBP regeneration may also be large (Fig. 3B,D). There is

618 supporting evidence as one of the slow-growing species in our study, *Banksia attenuata*,

619 with low photorespiration (Fig. 3C) was recently demonstrated to have low rRNA

620 concentrations in mature leaves at the Lesueur site (Sulpice *et al.* 2014). We believe that

621 the hypothesis of both N and P release in photorespiration establishes new significance

622 for what has previously been considered to be a "wasteful" process (Busch 2013; Ogren

623 1984; Wingler *et al.* 2000), but it also requires further investigation. There has been

624 considerable interest in the role of P in limiting photosynthesis and whether P can

625 directly influence leaf photosynthetic capacity (Reich *et al.* 2009). The relationships

626 between biochemical parameters underlying photosynthetic capacity and leaf P content

627 in Fig. 6 across a range in P supply argue for a stronger and more direct role for P in

628 regulating A_{max} in this set of species than for N. Our data have provided evidence of a

629 direct role of P in leaf photosynthetic capacity that is likely not currently realised much

630 since current C_i is often lower than ~ 28 Pa, but could become important with rising C_a.

631 Though the nature and biochemistry of T_p limitations to A_{max} are not fully elucidated,

632 when leaf P concentrations are moderate it appears that the extra photorespiratory

633 source of P_i derived from a net C export from the chloroplast can help sustain rapid

634 rates of A_{max}.

CONCLUSIONS

636 While triose-P utilisation (T_p) limitations to photosynthesis are considered to be

637 uncommon and are often ignored in photosynthetic model-fitting, we have shown that

638 T_p can be limiting in a wide range of species from across soil P gradients in the field,

639 with short-term high C_i. Hence, what are actually T_p limitations judged from

640 measurements at low pO_2, are currently attributed to J_{max} limitations in the two-phase

641 FvCB model that is frequently fit to measurements at normal pO_2. The results suggest

642 that pO_2 manipulation in measurements of A_{net} can lead to insights into P_i limitations to

643 A_{net} both in the present and in a future with elevated atmospheric CO_2 leading to

644 reduced photorespiration. Intracellular P_i release from photorespiration is inhibited at

645 low pO_2, reducing A_{max} in all species, but to varying extent depending on their available

646 P_i pools. Species with largest photosynthetic capacity and highest P_i contents apparently

647 rely most on ATP made available from photorespiration. Hence, this mechanism is most

648 important in fast-growing species at moderate P levels and with high photosynthetic

649 capacity, rather than species growing in P-impoverished soils. The mechanism we have

650 identified should be further explored, but is expected to contribute to the economy of P

651 for plants in tropical or subtropical rainforest vegetation as well as in Mediterranean

652 vegetation on soils with moderate to low P availability, but not in those species that

653 deploy alternative mechanisms to function at very low leaf [P]. Phosphate limitations to

654 photosynthetic capacity are likely more common in the field than previously thought,

655 and likely contribute to improving the predictability of CO_2-assimilation rates in such

656 instances. It is recommended that those interested in modelling how biochemistry

657 regulates A_{net} should consider the role of photorespiration and employ three limitations

658 in the biochemical model of photosynthesis with the possibility of glycerate not re-

659 entering the Calvin-Benson cycle.

675

676   **REFERENCES**

677   Aerts R. & Chapin F.S. (2000) The mineral nutrition of wild plants revisited: a re-

678   evaluation of processes and patterns. *Advances in Ecological Research*, **30**, 1-67.

679   Archontoulis S.V., Yin X., Vos J., Danalotos N.G. & Struick P.G. (2012) Leaf photosynthesis

680   and respiration of three bioenergy crops in relation to temperature and leaf

681   nitrogen: how conserved are biochemical model parameters among crop

682   species? *Journal of Experimental Botany*, **63**, 895–911.

683   Beadle N.C.W. (1966) Soil phosphate and its role in molding segments of the Australian

684   flora and vegetation, with special reference to xeromorphy and sclerophylly.

685   *Ecology*, **47**, 992-1007.

686   Beale S.I. (1978) Delta-aminolevulinic acid in plants - its biosynthesis, regulation, and

687   role in plastid development. *Annual Review of Plant Physiology and Plant*

688   *Molecular Biology*, **29**, 95-120.

689   Bernacchi C.J., Bagley J.E., Serbin S.P., Ruiz-Vera U.M., Rosenthal D.M. & Vanloocke A.

690   (2013) Modelling C3 photosynthesis from the chloroplast to the ecosystem. *Plant*

691   *Cell and Environment*, **36**, 1641–1657.

692   Bernacchi C.J., Singsaas E.L., Pimentel C., Portis A.R. & Long S.P. (2001) Improved

693   temperature response functions for models of Rubisco-limited photosynthesis.

694   *Plant Cell and Environment*, **24**, 253-259.

695   Bonan G.B., Lawrence P.J., Oleson K.W., Levis S., Jung M., Reichstein M., Lawrence D.M. &

696   Swenson S.C. (2011) Improving canopy processes in the Community Land Model

697 version 4 (CLM4) using global flux fields empirically inferred from FLUXNET

698 data. *Journal of Geophysical Research-Biogeosciences*, **116**.

699 Bown H.E., Watt M.S., Clinton P.W., Mason E.G. & Richardson B. (2009) Partititioning

700 concurrent influences of nitrogen and phosphorus supply on photosynthetic

701 model parameters of *Pinus radiata*. *Tree Physiology*, **27**, 335-344.

702 Brooks A. (1986) Effects of phosphorus nutrition on Ribulose-1,5-bisphosphate

703 carboxylase activation, photosynthetic quantum yield and amounts of some

704 Calvin-cycle metabolites in spinach leaves. *Australian Journal of Plant Physiology*,

705 **13**, 221-237.

706 Brown S.L., Warwick N.W.M. & Prychid C.J. (2013) Does aridity influence the

707 morphology, distribution and accumulation of calcium oxalate crystals in Acacia

708 (Leguminosae: Mimosoideae)? *Plant Physiology and Biochemistry*, **73**, 219-228.

709 Bunce J.A. (2002) Sensitivity of infrared water vapor analyzers to oxygen concentration

710 and errors in stomatal conductance. *Photosynthesis Research*, **71**, 273–276.

711 Burch D.E., Singleton E.B. & Williams D. (1962) Absorption line broadening in the

712 infrared. *Applied Optics*, **1**, 359-363.

713 Busch F.A. (2013) Current methods for estimating the rate of photorespiration in leaves.

714 *Plant Biology*, **15**, 648-655.

715 Campbell C.D. & Sage R.F. (2006) Interactions between the effects of atmospheric CO_2

716 content and P nutrition on photosynthesis in white lupin (*Lupinus albus* L.). *Plant*

717 *Cell and Environment*, **29**, 844-853.

718 Cernusak L.A., Hutley L.B., Beringer J., Holtum J.A. & Turner B.L. (2011) Photosynthetic

719 physiology of eucalypts along a sub-continental rainfall gradient in northern

720 Australia. *Agricultural and Forest Meteorology*, **151**, 1462-1470.

721   Close D.G. & Beadle C.L. (2004) Total, and chemical fractions, of nitrogen and

722   phosphorus in *Eucalyptus* seedling leaves: Effects of species, nursery fertiliser

723   management and transplanting. *Plant and Soil*, **259**, 85-95.

724   Conn S. & Gilliham M. (2010) Comparative physiology of elemental distributions in

725   plants. *Annals of Botany*, **105**, 1081-1102.

726   Crous K.Y., Quentin A.G., Lin Y.-S., Medlyn B.E., Williams D.G., Barton C.V.M. & Ellsworth

727   D.S. (2013) Photosynthesis of temperate *Eucalyptus globulus* trees outside their

728   native range has limited adjustment to elevated CO_2 and climate warming. *Global*

729   *Change Biology*, **19**, 3790–3807.

730   Denton M.D., Veneklaas E.J., Freimoser F.M. & Lambers H. (2007) *Banksia* species

731   (Proteaceae) from severely phosphorus-impoverished soils exhibit extreme

732   efficiency in the use and re-mobilization of phosphorus. *Plant Cell and*

733   *Environment*, **30**, 1557-1565.

734   Domingues T.F., Meir P., Feldpausch T., Saiz G., Venendaal E.M., Schrodt F., Bird M.,

735   Djagblety G., Hien F., Camapore H., Diallo A., Grace J. & Lloyd J. (2010) Co-

736   limitation of photosynthetic capacity by nitrogen and phosphorus in West Africa

737   woodlands. *Plant Cell and Environment*, **33**, 959-980.

738   Ellsworth D.S., Reich P.B., Naumburg E.S., Koch G.W., Kubiske M.E. & Smith S.D. (2004)

739   Photosynthesis, carboxylation and leaf nitrogen responses of 16 species to

740   elevated pCO_2 across four free-air CO_2 enrichment experiments in forest,

741   grassland and desert. *Global Change Biology*, **10**, 2121-2138.

742   Ellsworth D.S., Thomas R.B., Crous K.Y., Palmroth S., Ward E., Maier C., DeLucia E.H. &

743   Oren R. (2012) Elevated CO_2 affects photosynthetic responses in canopy pine and

744   subcanopy deciduous trees over 10 years: a synthesis from Duke FACE. *Global*

745   *Change Biology*, **18**, 223–242.

746 Evans J.R. (1989) Photosynthesis and nitrogen relationships in leaves of C3 plants. *Oecologia*, **78**, 9-19.

748 Farquhar G.D., Caemmerer S.V. & Berry J.A. (1980) A biochemical model of photosynthetic CO_2 assimilation in leaves of C3 species. *Planta*, **149**, 78-90.

750 Farquhar G.D., von Caemmerer S. & Berry J.A. (2001) Models of photosynthesis. *Plant Physiology*, **125**, 42-45.

752 Flexas J., Barbour M.M., Brendel O., Cabrera H.M., Carriqui M., Diaz-Espejo A., Douthe C., Dreyer E., Ferrio J.P., Gago J., Galle A., Galmés J., Kodama N., Medrano H., Niinemets Ü., Peguero-Pina J.J., Pou A., Ribas-Carbo M., Tomas M., Tosens T. & Warren C.R. (2012) Mesophyll diffusion conductance to CO_2: An unappreciated central player in photosynthesis. *Plant Science*, **193**, 70-84.

757 Franceschi V.R. & Nakata P.A. (2005) Calcium oxalate in plants: formation and function. *Annual Review of Plant Biology*, **56**, 41-71.

759 Galmés J., Flexas J., Keys A.J., Cifre J., Mitchell R.A.C., Madgwick P.J., Haslam R.P., Medrano H. & Parry M.A.J. (2005) Rubisco specificity factor tends to be larger in plant species from drier habitats and in species with persistent leaves. *Plant Cell and Environment*, **28**, 571-579.

763 Griffin E.A. & Burbidge A.A. (1990) Description of the region. In: *Nature Conservation, Landscape and Recreational Values of the Lesueur Area.* (eds A.A. Burbidge, S.D. Hopper, & D. Van Leeuwen), pp. 15-24. Environmental Protection Authority, Perth, WA Australia.

767 Groenendijk M., Dolman A.J., van der Molen M.K., Leuning R., Arneth A., Delpierre N., Gash J.H.C., Lindroth A., Richardson A.D., Verbeeck H. & Wohlfahrt G. (2011) Assessing parameter variability in a photosynthesis model within and between

770   plant functional types using global Fluxnet eddy covariance data. *Agricultural*

771   *and Forest Meteorology*, **151**, 22-38.

772 Gu L. & Sun Y. (2014) Artefactual responses of mesophyll conductance to CO_2 and

773   irradiance estimated with the variable J and online isotope discrimination

774   methods. *Plant Cell and Environment*, **37**, 1231-1249.

775 Hammond J.P. & White P.J. (2011) Sugar signaling in root responses to low phosphorus

776   availability. *Plant Physiology*, **156**, 1033-1040.

777 Harley P.C. & Sharkey T.D. (1991) An improved model of C_3 photosynthesis at high CO_2:

778   reversed O_2 sensitivity explained by lack of glycerate reentry into the

779   chloroplast. *Photosynthesis Research*, **27**, 169-178.

780 Havrir E.A. (1984) Oxalate metabolism by tobacco leaf discs. *Plant Physiology*, **75**, 505-

781   507.

782 Holford I.C.R. (1997) Soil phosphorus: its measurement, and its uptake by plants.

783   *Australian Journal of Soil Research*, **35**, 227-239.

784 Jacob J. & Lawlor D.W. (1993) In vivo photosynthetic electron transport does not limit

785   photosynthetic capacity in phosphate deficient sunflower and maize leaves. *Plant*

786   *Cell and Environment*, **16**, 785–795.

787 Joliffe P.A. & Tregunna E.B. (1968) Effect of temperature, CO_2 concentration, and light

788   intensity on oxygen inhibition of photosynthesis in wheat leaves. *Plant*

789   *Physiology*, **43**, 902-906.

790 Kattge J., Knorr W., Raddatz T. & Wirth C. (2009) Quantifying photosynthetic capacity

791   and its relationship to leaf nitrogen content for global-scale terrestrial biosphere

792   models. *Global Change Biology*, **15**, 976–991.

793 Laing W.A., Ogren W.L. & Hageman R.H. (1974) Regulation of soybean net
794   photosynthetic CO_2 fixation by interaction of CO_2, O_2, and ribulose 1,5-
795   diphosphate carboxylase. *Plant Physiology*, **54**, 678-685.

796 Lambers H., Brundrett M.C., Raven J.A. & Hopper S.D. (2010) Plant mineral nutrition in
797   ancient landscapes: high plant species diversity on infertile soils is linked to
798   functional diversity for nutritional strategies. *Plant and Soil*, **334**, 11–31.

799 Lambers H., Cawthray G.R., Giavalisco P., Kuo J., Laliberté E., Pearse S.J., Scheible W.R.,
800   Stitt M., Teste F. & Turner B.L. (2012) Proteaceae from severely phosphorus-
801   impoverished soils extensively replace phospholipids with galactolipids and
802   sulfolipids during leaf development to achieve a high photosynthetic
803   phosphorus-use-efficiency. *New Phytologist*, **196**, 1098-1108.

804 Lambers H., Clode P., Hawkins H.-J., Laliberté E., R.S. O., Reddell P., Shane M.W., Stitt M. &
805   Weston P. (2015) Metabolic adaptations of the non-mycotrophic Proteaceae to
806   soils with low phosphorus availability. In: *Phosphorus Metabolism in Plants in the*
807   *Post-genomic Era: From Gene to Ecosystem.* (eds W.C. Plaxton & H. Lambers), pp.
808   1-44. Wiley-Blackwell, London.

809 Li-Cor (2008) Using the Li-6400/Li-6400XT Portable Photosynthesis System. Li-Cor,
810   Lincoln, NE USA.

811 Long S.P. & Bernacchi C. (2003) Gas exchange measurements, what can they tell us
812   about the underlying limitations to photosynthesis? Procedures and sources of
813   error. *Journal of Experimental Botany*, **54**, 2393-2401.

814 Loustau D., Brahim M.B., Gaudillere J.-P. & Dreyer E. (1999) Photosynthetic responses to
815   phosphorus nutrition in two-year-old maritime pine seedlings. *Tree Physiology*,
816   **19**, 707-715.

817 Manter D.K. & Kerrigan J. (2004) A/C-i curve analysis across a range of woody plant

818   species: influence of regression analysis parameters and mesophyll conductance.

819   *Journal of Experimental Botany*, **55**, 2581-2588.

820 Matzek V. & Vitousek P.M. (2009) N : P stoichiometry and protein : RNA ratios in

821   vascular plants: an evaluation of the growth-rate hypothesis. *Ecology Letters*, **12**,

822   765-771.

823 Merchant A., Peuke A.D., Keitel C., Macfarlane C., Warren C.R. & Adams M.A. (2010)

824   Phloem sap and leaf δ^{13}C, carbohydrates, and amino acid concentrations in

825   *Eucalyptus globulus* change systematically according to flooding and water deficit

826   treatment. *Journal of Experimental Botany*, **61**, 1785–1793.

827 Niklas K.J., Owens T., Reich P.B. & Cobb E.D. (2005) Nitrogen / phosphorus leaf

828   stoichiometry and the scaling of plant growth. . *Ecology Letters*, **8**, 636–642.

829 Ogren W.L. (1984) Photorespiration: pathways, regulation, and modification. *Annual*

830   *Review of Plant Physiology*, **35**, 415-442.

831 Paul M.J. & Foyer C.H. (2001) Sink regulation of photosynthesis. *Journal of Experimental*

832   *Botany*, **52**, 1383-1400.

833 Piao S.L., Sitch S., Ciais P., Friedlingstein P., Peylin P., Wang X.H., Ahlstrom A., Anav A.,

834   Canadell J.G., Cong N., Huntingford C., Jung M., Levis S., Levy P.E., Li J.S., Lin X.,

835   Lomas M.R., Lu M., Luo Y.Q., Ma Y.C., Myneni R.B., Poulter B., Sun Z.Z., Wang T.,

836   Viovy N., Zaehle S. & Zeng N. (2013) Evaluation of terrestrial carbon cycle models

837   for their response to climate variability and to CO_2 trends. *Global Change Biology*,

838   **19**, 2117-2132.

839 Pieters A.J., Paul M.J. & Lawlor D.W. (2001) Low sink demand limits photosynthesis

840   under P_i deficiency. *Journal of Experimental Botany*, **52**, 1083-1091.

841   Pons T., Flexas J., von Caemmerer S., Evans J.R., Genty B., Ribas-Carbo M. & Brugnoli E.

842   (2009) Estimating mesophyll conductance to CO_2: methodology, potential errors,

843   and recommendations. *Journal of Experimental Botany*, **60**, 2217–2234.

844   Raven J.A. (2012) Protein turnover and plant RNA and phosphorus requirements in

845   relation to nitrogen fixation. *Plant Science*, **188**, 25-35.

846   Reich P.B., Oleksyn J. & Wright I.J. (2009) Leaf phosphorus influences the

847   photosynthesis-nitrogen relation: a cross-biome analysis of 314 species.

848   *Oecologia*, **160**, 207-212.

849   Reumann S. & Weber A.P.M. (2006) Plant peroxisomes respire in the light: some gaps of

850   the photorespiratory C_2 cycle have become filled - others remain. *Biochim*

851   *Biophys Acta*, **1763**, 1496–1510.

852   Rogers A. (2014) The use and mis-use of $V_{c,max}$ in earth system models. *Photosynthesis*

853   *Research*, **119**, 15-29.

854   Sage R.F. & Sharkey T.D. (1987) The effect of temperature on the occurrence of O_2 and

855   CO_2-insensitive photosynthesis in field grown plants. *Plant Physiology*, **84**, 658-

856   664.

857   Sharkey T.D. (1985) Photosynthesis in intact leaves of C3 plants - physics, physiology

858   and rate limitations. *Botanical Review*, **51**, 53-105.

859   Sharkey T.D. (1988) Estimating the rate of photorespiration in leaves. *Physiologia*

860   *Plantarum*, **73**, 147-152.

861   Sharkey T.D., Bernacchi C.J., Farquhar G.D. & Singsaas E.L. (2007) Fitting photosynthetic

862   carbon dioxide response curves for C3 leaves. *Plant Cell and Environment*, **30**,

863   1035-1040.

864   Sharkey T.D. & Vassey T.L. (1989) Low oxygen inhibition of photosynthesis is caused by

865   inhibition of starch synthesis. *Plant Physiology*, **90**, 385-387.

866   Stitt M., Lunn J. & Usadel B. (2010) *Arabidopsis* and primary photosynthetic metabolism

867   – more than the icing on the cake. *Plant Journal*, **61**, 1067-1091.

868   Sulpice R., Ishihara H., Schlereth A., Cawthray G.R., Encke B., Giavalisco P., Ivakov A.,

869   Arrivault S., Jost R., Krohn N., Kuo J., Laliberte E., Pearse S.J., Raven J.A., Scheible

870   W.R., Teste F., Veneklaas E.J., Stitt M. & Lambers H. (2014) Low levels of

871   ribosomal RNA partly account for the very high photosynthetic phosphorus-use

872   efficiency of Proteaceae species. *Plant Cell and Environment*, **37**, 1276-1298.

873   Tazoe Y., von Caemmerer S., Estavillo G.M. & Evans J.R. (2011) Using tunable diode laser

874   spectroscopy to measure carbon isotope discrimination and mesophyll

875   conductance to CO_2 diffusion dynamically at different CO_2 concentrations. *Plant*

876   *Cell and Environment*, **34**, 580-591.

877   R Core Development Team (2014) A language and environment for statistical

878   computing. R Foundation for Statistical Computing, Vienna, Austria.

879   http://www.R-project.org.

880   Thomas D.S., Montagu K.D. & Conroy J.P. (2006) Leaf inorganic phosphorus as a

881   potential indicator of phosphorus status, photosynthesis and growth of

882   *Eucalyptus grandis* seedlings. *Forest Ecology and Management*, **223**, 267–274.

883   Veneklaas E.J., Lambers H., Bragg J., Finnegan P.M., Lovelock C.E., Plaxton W.C., Price

884   C.A., Scheible W.R., Shane M.W., White P.J. & Raven J.A. (2012) Opportunities for

885   improving phosphorus-use efficiency in crop plants. *New Phytologist*, **195**, 306-

886   320.

887   Vitousek P.M., Porder S., Houlton B.Z. & Chadwick O.A. (2010) Terrestrial phosphorus

888   limitation: mechanisms, implications, and nitrogen-phosphorus interactions.

889   *Ecological Applications*, **20**, 5-15.

890   von Caemmerer S. (2000) *Biochemical Models of Leaf Photosynthesis.* CSIRO Publishing,

891   Collingwood, Victoria, Australia.

892   von Caemmerer S. (2013) Steady-state models of photosynthesis. *Plant Cell and*

893   *Environment*, **36**, 1617-1630.

894   von Caemmerer S. & Farquhar G.D. (1981) Some relationships between the

895   biochemistry of photosynthesis and the gas exchange of leaves. *Planta*, **153**, 376-

896   387.

897   Walker A.P., Beckerman A.P., Gu L., Kattge J., Cernusak L.A., Domingues T.F., Scales J.C.,

898   Wohlfahrt G., Wullschleger S.D. & Woodward F.I. (2014) The relationship of leaf

899   photosynthetic traits - Vcmax and Jmax - to leaf nitrogen, leaf phosphorus, and

900   specific leaf area: a meta-analysis and modeling study. *Ecology and Evolution*, **4**,

901   3218-3235.

902   Walker B., Ariza L.S., Kaines S., Badger M.R. & Cousins A.B. (2013) Temperature

903   response of *in vivo* Rubisco kinetics and mesophyll conductance in *Arabidopsis*

904   *thaliana*: comparisons to *Nicotiana tabacum*. *Plant Cell and Environment*, **36**,

905   2108-2119.

906   Wang Y.P., Law R.M. & Pak B. (2010) A global model of carbon, nitrogen and phosphorus

907   cycles for the terrestrial biosphere. *Biogeosciences*, **7**, 2261-2282.

908   Williams M., Rastetter E.B., Fernandes D.N., Goulden M.L., Shaver G.R. & Johnson L.C.

909   (1997) Predicting gross primary productivity in terrestrial ecosystems.

910   *Ecological Applications*, **7**, 882-894.

911   Wingler A., Lea P.J., Quick W.P. & Leegood R.C. (2000) Photorespiration: metabolic

912   pathways and their role in stress protection. *Philosophical Transactions of the*

913   *Royal Society London Series B*, **355**, 1517-1529.

914   Yang X. & Post W.M. (2011) Phosphorus transformations as a function of pedogenesis: a

915   synthesis of soil phosphorus data using Hedley fractionation method.

916   *Biogeosciences*, **8**, 2907-2916.

917   Zaehle S., Medlyn B.E., De Kauwe M.G., Walker A.P., Dietze M.C., Hickler T., Luo Y.Q.,

918   Wang Y.P., El-Masri B., Thornton P., Jain A., Wang S.S., Warlind D., Weng E.S.,

919   Parton W., Iversen C.M., Gallet-Budynek A., McCarthy H., Finzi A., Hanson P.J.,

920   Prentice I.C., Oren R. & Norby R.J. (2014) Evaluation of 11 terrestrial carbon-

921   nitrogen cycle models against observations from two temperate Free-Air CO_2

922   Enrichment studies. *New Phytologist*, **202**, 803-822.

923

924

Table 1. Description of species and sites included in the study along with number of individuals measured (N), the mean height that measurements were taken at, and the mean leaf thickness, leaf dry mass-to-area ratio, and total leaf P concentration per unit leaf area (P_a). Data are means ± s.e. The species name abbreviation is used to denote the different species in the figures.

Species name and abbrev.	Type	Site	Location	N	Height (m)	Leaf thickness (µm)	M_a (g m^{-2})	Leaf P_a (mmol P m^{-2})
Acacia oblongifolia (A. obl)	Native shrub	Davies Park, Springwood, NSW	33º 42' 28" S, 150º 32' 51" E	4	1-2	315	192.5 ± 11.8	2.5 ± 0.5
Banksia attenuata (B. att)	Native shrub	Lesueur National Park, Jurien Bay, WA	30º 11' 02" S, 115º 09' 27" E	3	1	430	271.5 ± 19.5	2.7 ± 0.4
B. serrata (B. ser)	Native shrub	Davies Park, Springwood, NSW	33º 42' 28" S, 150º 32' 51" E	3	1-2	540	207.2 ± 3.7	1.7 ± 0.2
Eucalyptus dunnii (E. dun)	Plantation tree	Hawkesbury Forest Experiment, Richmond NSW	33º 36' 40" S, 150º 44' 27" E	4	10	260	135.6 ± 2.6	6.1 ± 0.5
E. fastigata (E. fas)	Native mature sclerophyll woodland tree	Illawarra escarpment, Robertson, NSW	34° 37' 06" S, 150° 42' 48" E	5	25	300	168.9 ± 10.3	8.2 ± 1.6
E. saligna (E. sal)	Plantation tree	Hawkesbury Forest Experiment, Richmond NSW	33º 36' 40" S, 150º 44' 27" E	3	9	318	147.2 ± 7.3	6.3 ±1.7
E. tereticornis (E. ter)	Native mature sclerophyll woodland tree	Eucalyptus site (EucFACE), Richmond, NSW	33º 36' 57" S, 150º 44' 16" E	3	19	356	208.3 ± 11.7	7.3 ± 0.3
E. todtiana (E. tod)	Native mature woodland tree	Lesueur National Park, Jurien Bay, WA	30º 11' 02" S, 115º 09' 27" E	3	2	530	305.0 ± 4.5	3.8 ± 0.4
Liquidambar styraciflua (L. sty)	Plantation tree	Hawkesbury campus, Richmond, NSW	33º 36' 57" S, 150º 45' 06" E	4	4	237	111.9 ± 2.0	6.6 ±1.5

| *Persoonia levis* (P. lev) | Native shrub | Davies Park, Springwood, NSW | 33º 42' 28" S, 150º 32' 51" E | 4 | 2 | 420 | 167.0 ± 18.8 | 1.8 ± 0.1 |

Table 2. Summary of relationships between biochemical parameters of leaf photosynthetic capacity and leaf chemistry for ten species in this study. Leaf N_{area} and P_{area} are expressed in mmol m^{-2}.

Relationship	Equation	Coefficient of determination (R^2)	P-value
V_{cmax} by N_{area}	N.S.	-	0.874
V_{cmax} by P_{area}	N.S.	0.371	0.062
V_{omax} by N_{area}	N.S.	-	0.361
V_{omax} by P_{area}	$V_{omax} = 27.66 + 3.54*P_{area}$	0.394	0.052
J_{max} by N_{area}	N.S.	-	0.322
J_{max} by P_{area}	$J_{max} = 88.56 + 400.99*P_{area}$	0.656	0.045
T_p by N_{area}	N.S.	-	0.201
T_p by P_{area}	$T_p = 6.51 + 14.64*P_{area}$	0.446	0.035

Figure 1. Diagram of the biochemical models hypothesised to account for the O_2 sensitivity of photosynthesis, with emphasis placed on areas indicated by the encircled as A) showing limitations by end-product synthesis (depicted in Eqn 6), and the circle B) showing the hypothesised mechanism from Harley & Sharkey (1991) with emphasis on P_i release by P-glycolate phosphatase and subsequent incomplete photorespiratory glycerate re-entry to the chloroplast (depicted in Eqn 7), resulting in a net increase in stromal P_i for photophosphorylation and RuBP regeneration. The small boxes are membrane-bound transporters.
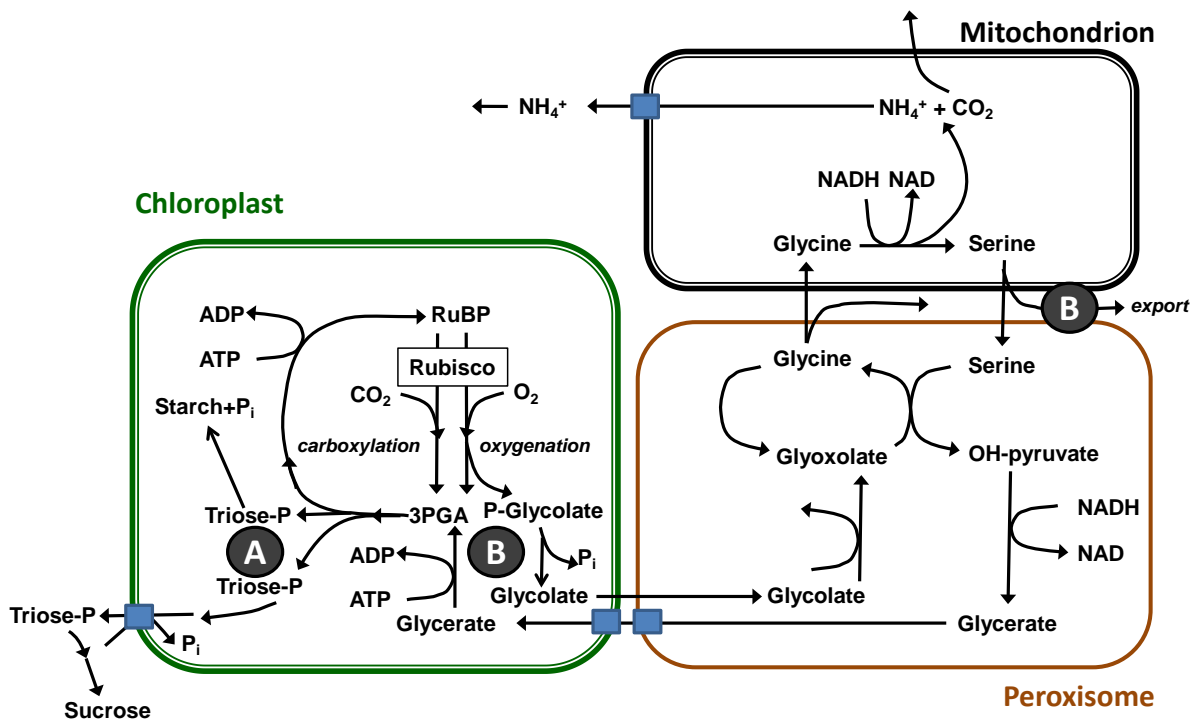
Figure 2. A theoretical depiction of the prediction of A_{net} as a function of the CO_2 partial pressure inside the chloroplast (C_c) (a) for normal O_2 and (b) for low pO_2 predicted by the biochemical model of FvCB, showing the component limitations to A_{net} in colour. Blue dashes show the theoretical A_{net} limited by the maximum capacity for carboxylation, orange dashes shows the theoretical A_{net} limited by electron transport for the regeneration of RuBP in the Calvin-Benson cycle, and green dashes show the theoretical A_{net} limited by triose-phosphate utilisation as per Eqn 6. The dark black line shows the overall relationship between A_{net} and C_c predicted by the minimum of the three limitations. The grey line in (b) represents the black curve in (a) for direct comparison with predictions for low pO_2.
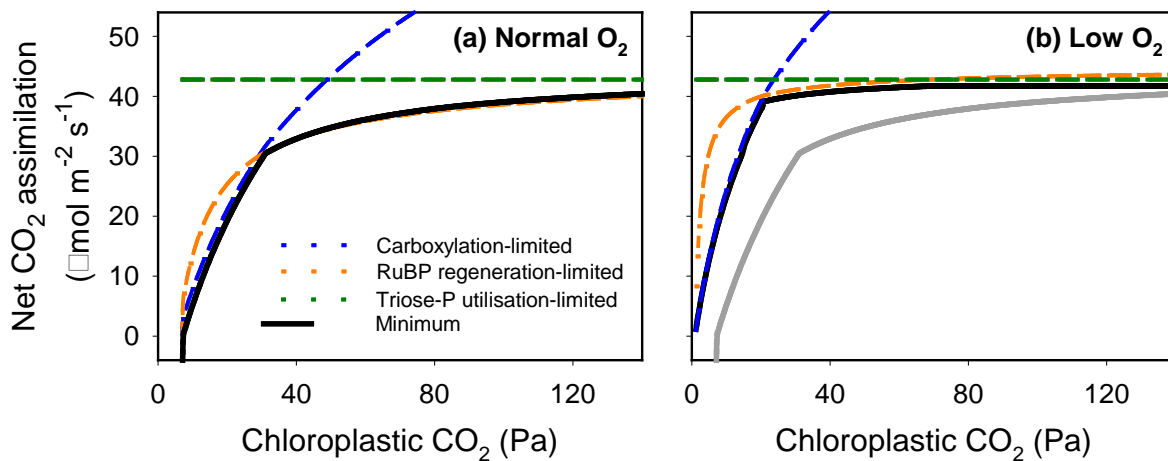
Figure 3. A_{net} as a function of chloroplastic pCO_2 partial pressure (C_c) measured in the field for four woody species examples (*P. levis*, *B. attenuata*, *L. stryraciflua*, and *E. fastigata*, panels a-d, respectively) at both normal (21 kPa, filled light blue symbols) and low pO_2 (2 kPa, open red symbols), with ensemble response curve fits for each species and pO_2 level. Data are for three to four leaves from different trees on which measurements at both pO_2 values had been made (see Table 1). The lines shown represent separate fits of the standard model of Farquhar *et al.* (1980) to all the data at each respective pO_2 for a given species.
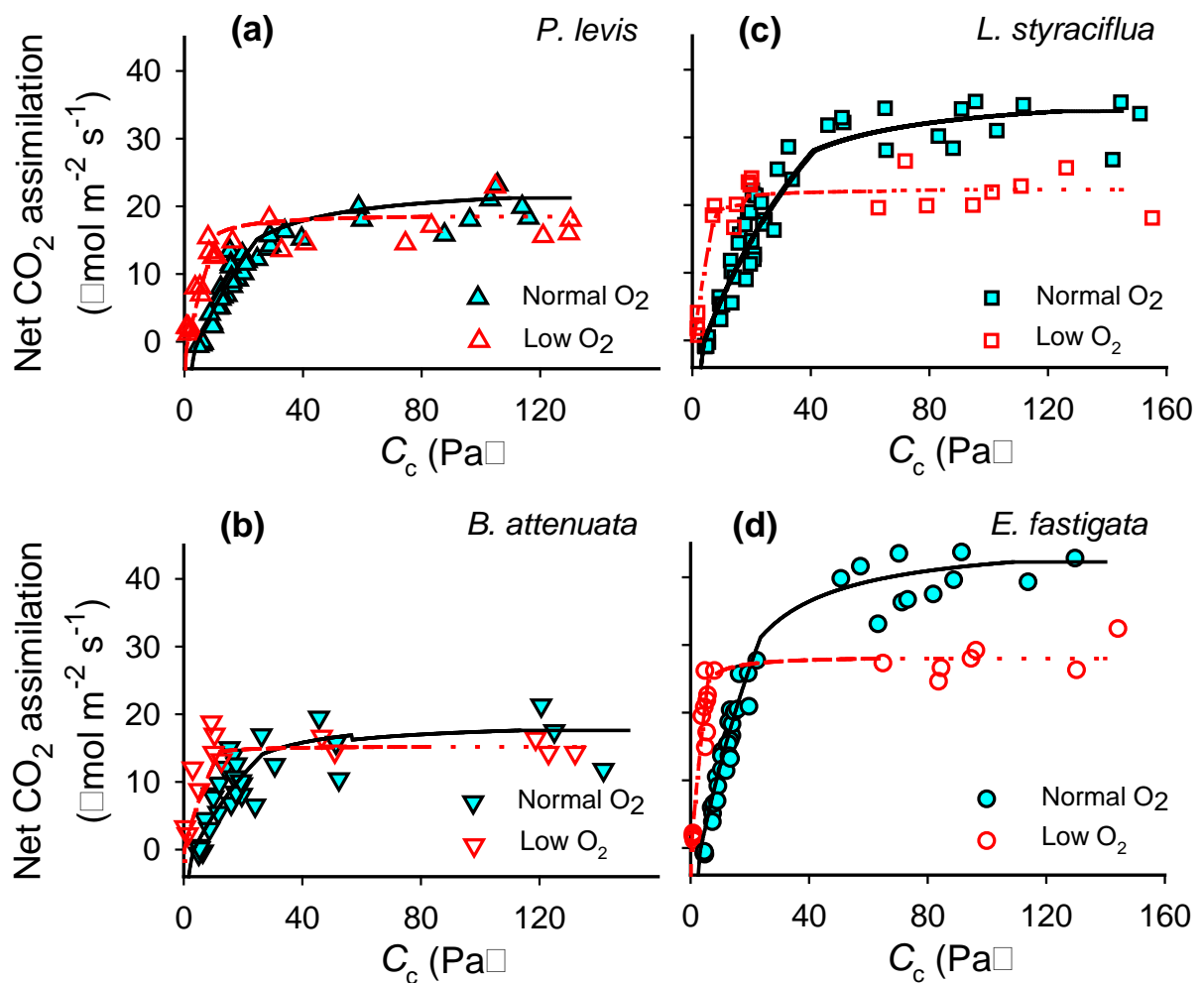
Figure 4. Results of the independent fits of the standard Farquhar *et al.* (1980) model to data at normal versus at low pO_2 for ten species for a) carboxylation capacity (V_{cmax}), b) light- and CO_2-saturated photosynthetic capacity (A_{max}), and c) the A_{max} difference in low pO_2 modelled including T_p limitation versus not including T_p limitation as a function of A_{max} in normal pO_2. Panel (d) shows A_{max} in low pO_2 modelled including T_p limitation as a function of A_{max} measured in normal pO_2. The 1:1 line in panels a,b,d is shown as a dashed line across each panel and the solid line in panel c represents the line delineated by $Y = 0.50*x - 6.83$, with $r^2 = 0.79$. Species are abbreviated to four letters representing the genus and species names (see Table 1).

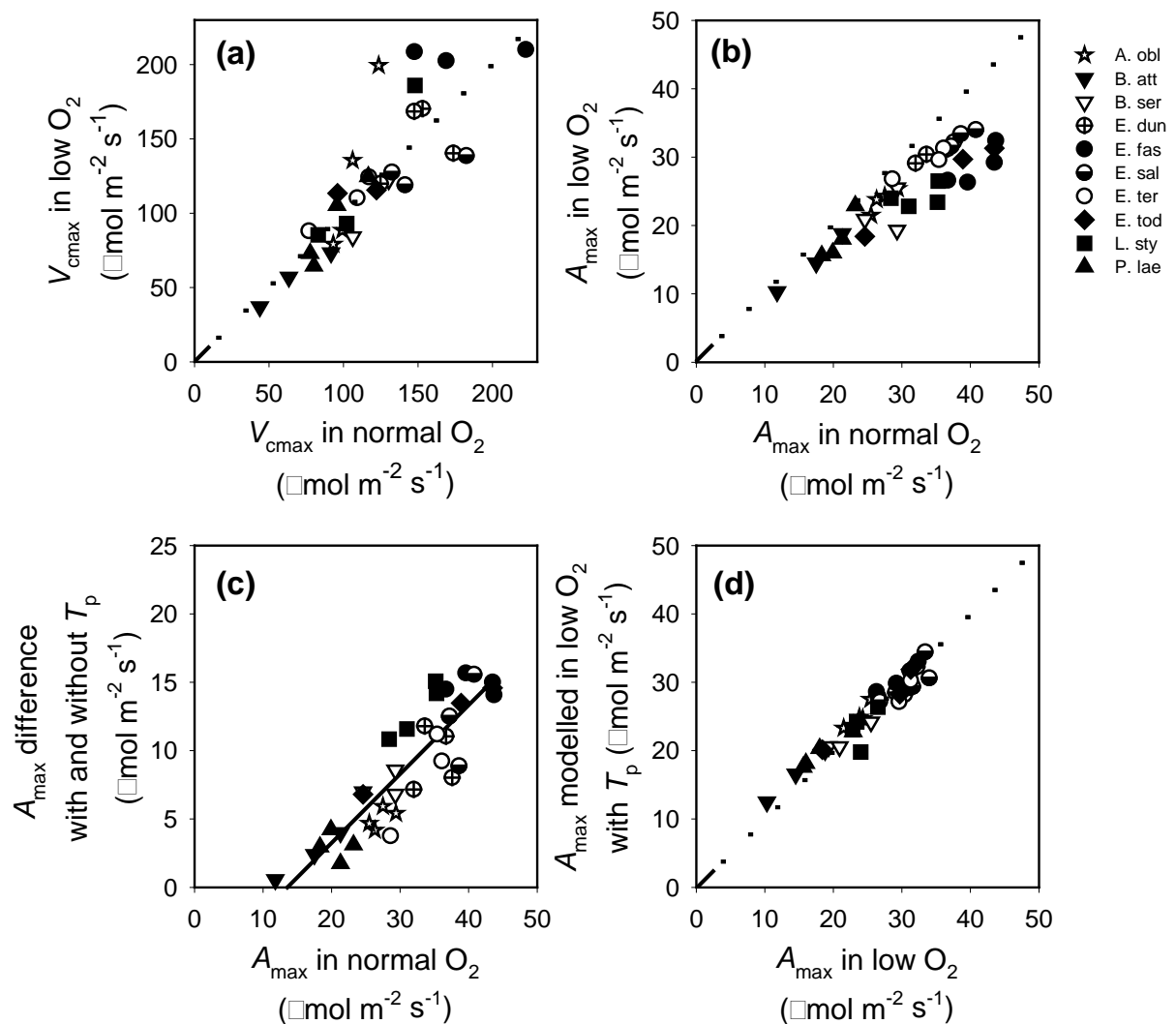**Figure 5**. The difference in A_{max} in low pO_2 when modelled including T_p limitation from Eqn 7 versus A_{max} in low pO_2 without T_p limitation considered is shown as a function of bulk leaf inorganic P, P_i. Species abbreviations are given in Table 1.
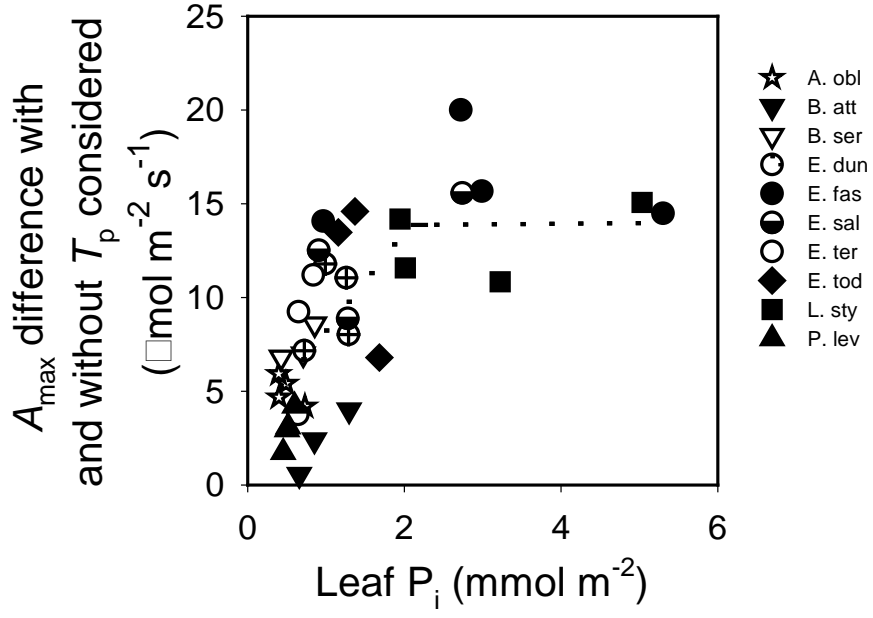
Figure 6. The relationships between four modelled biochemical components of photosynthetic or photorespiratory capacity (V_{cmax}, panel a; V_{omax}, panel b; J_{max}, panel c; T_p, panel d) and leaf P concentration for the ten species studied (abbreviation in Table 1). Each point represents the mean of individuals of a species (see Table 1), fit ensemble. V_{cmax} and V_{omax} species means across different individuals are reported in Supporting Information, Table S1. Dashed lines are shown where the relationships are significant. The data point for *Acacia obtusifolia* is obscured by that of *Banksia serrata* in panel C, as they had very similar J_{max} values. Equations for these relationships are shown in Table 2.
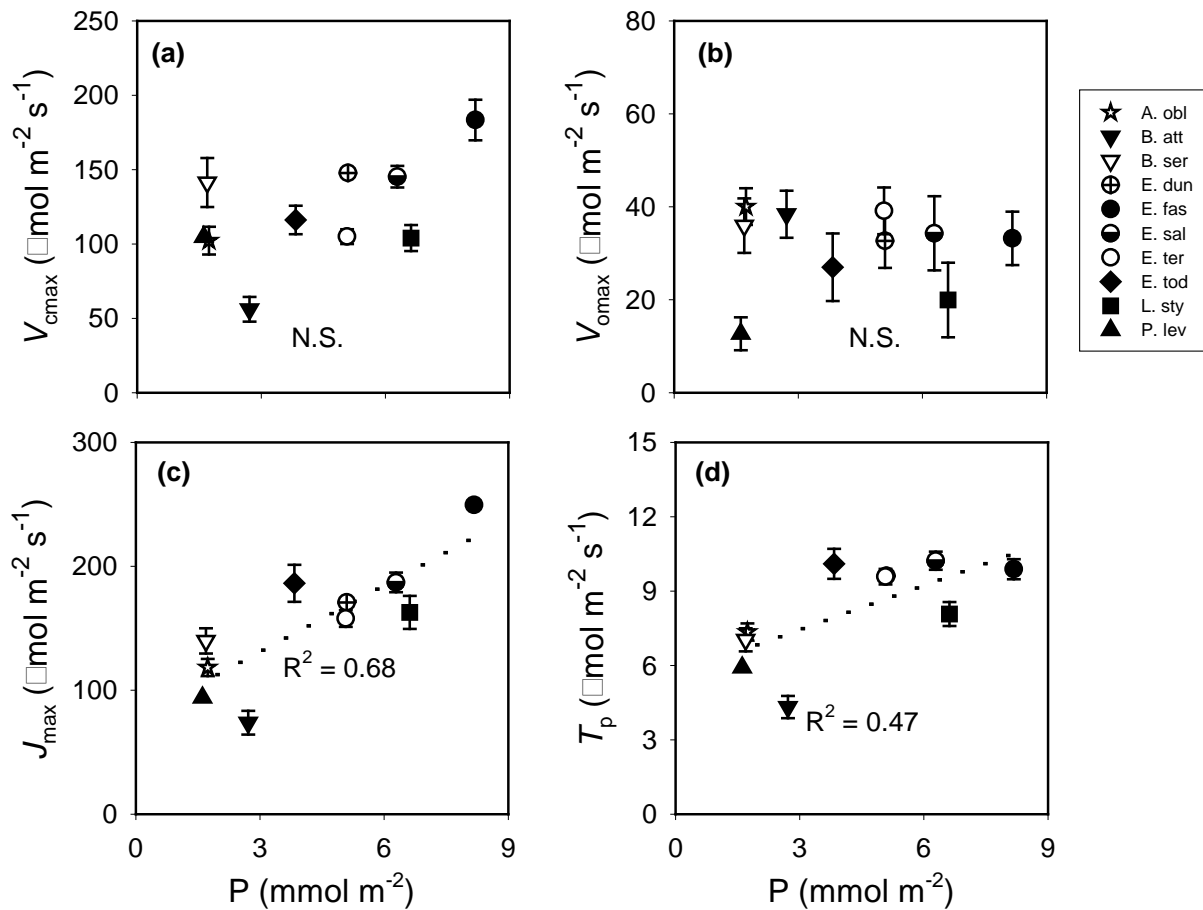
Supporting Information

Table S1. Summary of species means for V_{cmax}, fit using both pO_2 levels up to a C_c threshold of 18 Pa, V_{omax} as a measure of photorespiratory capacity, also fit from data from both pO_2 up to a C_c threshold of 18 Pa, and leaf N and P concentrations and N to P ratios for the ten species in this study. Data are means ± s.e.

Species name	V_{cmax} (μmol CO_2 m^{-2} s^{-1})	V_{omax} (μmol CO_2 m^{-2} s^{-1})	Leaf N (mg N g^{-1})	Leaf P (mg P g^{-1})	N:P
Acacia oblongifolia	109.8 ± 14.9	40.1 ± 3.9	17.8 ± 2.0	0.31 ± 0.10	67
Banksia attenuata	63.8 ± 11.5	38.4 ± 5.1	11.3 ± 1.4	0.31 ± 0.6	39
B. serrata	129.2 ± 23.5	35.9 ± 5.9	6.5 ± 0.5	0.25 ± 0.03	27
Eucalyptus dunnii	163.5 ± 6.1	32.7 ± 5.8	19.2 ± 1.1	1.18 ± 0.04	16
E. fastigata	204.6 ± 12.6	33.2 ± 5.7	18.0 ± 0.5	1.50 ± 0.28	13
E. saligna	144.7 ± 3.5	34.3 ± 8.0	21.3 ± 1.2	1.35 ± 0.39	19
E. tereticornis	100.7 ± 18.0	39.1 ± 5.0	16.3 ± 0.7	0.78 ± 0.09	21
E. todtiana	118.4 ± 10.3	27.0 ± 7.3	11.8 ± 1.1	0.38 ± 0.05	32
Liquidambar styraciflua	138.4 ± 22.3	20.0 ± 8.0	17.7 ± 1.4	1.83 ± 0.42	11
Persoonia levis	100.1 ± 13.9	12.7 ± 3.5	7.8 ± 0.3	0.30 ± 0.04	24

Figure S1. Time series of measurements of A_{net} before, during and after a pulse of low pO$_2$ was delivered to the leaf chamber for two *Eucalyptus* species (a, b). At the flow rate used, 65 sec was the time constant for mixing. Data shown are examples from (a) *Eucalyptus todtiana* measured at Lesueur National Park in Western Australia, and (b) *E. tereticornis* measures at EucFACE in NSW, Australia, for measurements at a C_a of 40 Pa. The final measurement in low pO$_2$ before switching O$_2$ back to normal pO$_2$ was considered at equibilibrium and was used in the calculations.